

Ultrasound Stimulation Attenuates CRS-Induced Depressive Behavior by Modulating Dopamine Release in the Prefrontal Cortex

Ling Wang¹, Sutong Wang, Weiyi Mo¹, Yaqing Li, Qing Yang, Yutao Tian, Chenguang Zheng, Jiajia Yang¹, and Dong Ming¹, *Senior Member, IEEE*

Abstract—Depression is one of the most serious mental disorders affecting modern human life and is often caused by chronic stress. Dopamine system dysfunction is proposed to contribute to the pathophysiology of chronic stress, especially the ventral tegmental area (VTA) which mainly consists of dopaminergic neurons. Focused ultrasound stimulation (FUS) is a promising neuromodulation modality and multiple studies have demonstrated effective ultrasonic activation of cortical, subcortical, and related networks. However, the effects of FUS on the dopamine system and the potential link to chronic stress-induced depressive behaviors are relatively unknown. Here, we measured the effects of FUS targeting VTA on the improvement of depression-like behavior and evaluated the dopamine concentration in the downstream region - medial prefrontal cortex (mPFC). We found that targeting VTA FUS treatment alleviated chronic restraint stress (CRS) -induced anhedonia and despair behavior. Using an in vivo photometry approach, we analyzed the dopamine signal of mPFC and revealed a significant increase following the FUS, positively associated with the improvement of anhedonia behavior. FUS also protected the dopaminergic neurons in VTA from the damage caused by CRS exposure. Thus, these results demonstrated that targeting VTA FUS treatment significantly rescued the depressive-like behavior and declined dopamine level of mPFC induced by CRS. These beneficial effects of FUS might be due to protection in the DA neuron of VTA. Our

findings suggest that FUS treatment could serve as a new therapeutic strategy for the treatment of stress-related disorders.

Index Terms—Depression, chronic stress, dopamine, VTA, mPFC, focused ultrasound stimulation.

I. INTRODUCTION

DEPRESSIVE disorder is a significant public and debilitating neurobiological illness that affects approximately 17% of the world's population in a lifetime, and is associated with high suicidal risk and serious economic burden [1]. A tremendous number of studies have established that stress is a crucial factor in mental disorder, particularly the development of depression [2], [3]. Stress exposure to mice can induce despair and altered responses to reward, which are characteristic symptoms of depression in humans [4]. However, the etiology and pathophysiology of chronic stress-inducing depression remain not clear.

The mesolimbic dopaminergic system is known as a major reward-related center in the brain [5], [6]. Changes in dopaminergic neurotransmission can modify and alter behavioral responses to different environmental stimuli [5]. Dopaminergic cells are mainly located in the ventral tegmental area (VTA) which is located in the midbrain, with DA neurons comprising 65% of the area [7], [8]. DAergic neurons from VTA project to numerous different areas of the brain to regulate behaviors through mediating dopamine release in the downstream regions, including the medial prefrontal cortex (mPFC), hippocampus, nucleus accumbens, and amygdala [9]. mPFC is a key part of the brain networks that involve reward, and social behavior [10], [11]. The decrease in dopamine levels was observed in the mPFC of depression mice model [2]. Meanwhile, enhancing the DA level in mPFC can induce antidepressant (-like) effects in both naïve and stress depressive animal models [12]. However, the role of VTADA projecting to the mPFC in stress-related emotions and mood disorders is currently unknown.

Focused ultrasound stimulation (FUS), an emerging non-invasive neuromodulation, has been rapidly developed with the advantage of excellent targeting, penetration depth, and spatial resolution [13], [14], [15]. Among previous animal reports, low-intensity FUS has been proven to be useful in

Manuscript received 11 November 2023; revised 19 February 2024; accepted 8 March 2024. Date of publication 19 March 2024; date of current version 26 March 2024. This work was supported in part by the National Key Research and Development Program of China under Grant 2023YFF1204004 and in part by the National Natural Science Foundation of China under Grant 82371886 and Grant 82202797. (Ling Wang and Sutong Wang contributed equally to this work.) (Corresponding authors: Jiajia Yang; Dong Ming.)

This work involved human subjects or animals in its research. Approval of all ethical and experimental procedures and protocols was granted by the Ethical Committee of the Tianjin University under Approval No. TJUE-2022-095, March 9, 2022.

Ling Wang, Yutao Tian, Chenguang Zheng, Jiajia Yang, and Dong Ming are with the Academy of Medical Engineering and Translational Medicine, Tianjin University, Tianjin 300072, China, also with Tianjin Key Laboratory of Brain Science and Neuroengineering, Tianjin 300072, China, and also with the Haihe Laboratory of Brain-Computer Interaction and Human-Machine Integration, Tianjin 300072, China (e-mail: jiajia.yang@tju.edu.cn; richardming@tju.edu.cn).

Sutong Wang, Weiyi Mo, Yaqing Li, and Qing Yang are with the Academy of Medical Engineering and Translational Medicine, Tianjin University, Tianjin 300072, China.

Digital Object Identifier 10.1109/TNSRE.2024.3378976

treating various neurological and psychiatric diseases such as social dysfunction [16], brain ischemic [17], Parkinson's disease [18], and depression [13]. Although the mechanisms of ultrasound stimulation remain unclear, many studies suggest that the US can enhance neuron activity and the release of neurotransmitters [13], [19], [20]. Therefore, ultrasound stimulation targeting VTA may enhance the dopamine levels of mPFC to improve stress-induced depression-like behaviors.

Here, we report that FUS regulation could improve depression-like behavior induced by CRS. Targeting VTA by FUS may regulate the dopamine system of CRS mice and increase the concentration of dopamine in the downstream mPFC. FUS regulation could ameliorate the structural damage of neurons caused by CRS and increase the number of dopamine neurons in VTA. These results provided an experimental and theoretical basis for FUS to improve depression-like behavior and provided new ideas for exploring the prevention and treatment of stress-induced depression.

II. MATERIALS AND METHODS

A. Animals

All mice were purchased from the Beijing Vital River Laboratory Animal Technology Co. Ltd. Eight- to twelve-week-old female mice were used for experiments. The mice were group housed (4-5) in home cages on a 12-h light/dark cycle at 23-25 °C with food and water continuously available. The light cycle was from 8 a.m. to 8 p.m. All of the animal procedures were approved by the Animal Care and Use Committee of the Tianjin Hospital of Tianjin University. All efforts were made to minimize the number of animals and their suffering.

B. Stereotactic Surgeries

Before surgery, general anesthesia was induced by placing the mice in a transparent anesthetic chamber filled with 3-5 % isoflurane. The anesthesia was maintained during surgery with 1-2 % isoflurane applied to the nostrils of the mice using a precision vaporizer. Mice were checked for the absence of the tail-pinch reflex as a sign of sufficient anesthesia. The mice were then immobilized in a stereotaxic frame (RWD Life Science Co. Ltd, China), and erythromycin eye ointment was applied to prevent eye drying. After an incision was made along the midline of the scalp, unilateral or bilateral craniotomies were performed using a microdrill with 0.5 mm burrs. The tips of glass capillaries loaded with the virus-containing solution were placed into the prelimbic division of the mPFC (1.8 mm rostral to bregma, 0.3 mm lateral to the midline, and 2.0 mm ventral to the pial surface). Virus-containing solution was injected at a rate of 0.1 μ l/min using a 1 μ l Hamilton microsyringe and a syringe pump (KD Scientific, USA). The total volume of GPCR activation-based-DA was 0.35 μ l for AAV2/9-hSyn-DA4.4-WPRE-hGH pA (BrainVTA Co. Ltd, China).

C. Chronic Restraint Stress Model

Put the mouse into a 50-ml centrifuge tube, which owned several ventilators distributed on the bottle body. Animals

can keep free breathing, but cannot move a step. The mouse is bound for 4 hours every day during the waking time to ensure that each mouse is bound for the same time. While the CRS group mice were restrained, the CON group mice were deprived of food and water. After a 4-week continuous restraint, the modeling mice were randomly divided into the non-FUS group (CRS group) and the FUS group (CRS+FUS group).

D. Focused Ultrasound Stimulation

The ultrasound stimulation system consists of two function generators (DG4162 and DG822, RIGOL, China), a custom-designed radio frequency amplifier (SWA400A, North Star, China), a 0.5 MHz single-element immersion transducer (V318, Olympus, USA), and a custom-designed acoustic collimator. The FUS parameters applied to chronic stimulation were as follows: 0.5 MHz center frequency, 1.5 kHz pulse repetition frequency, 150 cycles, 0.3-ms tone burst duration, 0.2-s sonication duration, 1.6-s stimulation interval, and 150 mW/cm² spatial peak temporal average intensity (I_{spta}). A custom-made, cone-shaped plastic housing was combined with the ultrasound transducer and filled with degassed water for transmitting acoustic waves. During the FUS stimulation, mice were anesthetized by isoflurane and positioned on a stereotaxic apparatus. The ultrasound transducer was affixed above the mouse head at an angle of 30° to the surface of the skull (60° to the coronal plane) so that the focal zone of the transducer targeted the VTA region. The FUS procedure was performed for 15 min each day for 10 days. Mice in CON and CRS groups were anesthetized by isoflurane and experienced sham stimulation. They were applied with ultrasound gel over the scalp but placed 5 cm away from the ultrasound transducer so that there was no ultrasound stimulation in these sham groups.

To evaluate the transcranial attenuation of ultrasound, we fixed the collimator with a fresh mouse skull covered with dental cement at the same angle as that for real stimulation as described above. A signal was generated by a 150-cycle pulse of 0.5 MHz ultrasound. The acoustic intensity field was measured in a degassed water tank by a calibrated hydrophone (NH4000, Precision acoustics, Dorchester, United Kingdom). To determine the output acoustic distribution on X-Y and X-Z planes, the hydrophone was placed at the focal zone of ultrasound and was scanned every 1 mm. The calculation showed the decay ratio was about 40%, thus the I_{spta} delivering to the targeted region-VTA was around 90 mW/cm².

E. Behavioral Procedures

On the test day, mice were transferred to the testing room and acclimated to the room conditions for at least 1 h. After each test session, the apparatus was thoroughly cleaned with 75% alcohol and tap water to eliminate the previously tested mouse's odor and trace.

1) *Sucrose Preferences Test*: Before the SPT, mice were trained to habituate 1% sucrose water by placing a bottle of normal water and a bottle of sucrose solution with them for one day. Afterward, they were deprived of food and water for 24 hours. Then start the experiment, mice were

singly housed and given access to two bottles (containing water or 1% sucrose) for 2 h. The water and sucrose bottle positions were switched every 1 h to ensure that the mice did not develop a side preference. After this period, mice were left undisturbed, and their overnight fluid consumption was measured the next morning (8:00 a.m.). Sucrose preference was calculated as a percentage (amount of sucrose consumed (bottle A) \times 100/total volume consumed (bottles A + B)). Then the SPI change relative to the CON was calculated and analyzed.

2) *Tail Suspension Test*: Mice were suspended by tails with medical adhesive tape 1 cm from the tip of the tail. The behavior was videotaped from the side for 6 min. The immobility time was analyzed during the last 4 min of the 6-min test session. Immobility was defined as no movement at all and hanging down passively.

3) *Forced Swimming Test*: Mice were gently placed in a transparent glass cylinder (diameter 10 cm, height 25 cm) of water (25 °C, 15 cm in height) under bright light conditions and videotaped for 6 min. The immobility time was analyzed during the last 4 min of a 6-min test session. Immobility was defined as no movement at all or only minor movements necessary to keep the nose above the water versus mobility, which was defined by swimming and struggling behaviors.

4) *Novelty-Suppressed Feeding Test*: After 24 h of food deprivation and water available ad libitum, mice were placed in a brightly lit open arena (40 \times 40 \times 40 cm). A familiar food pellet was placed in the center of the arena. Mice were removed from their home cage, and placed in a corner of the testing arena to explore freely at most 10 min. The latency to begin a feeding episode was recorded with a video camera suspended above the arena and saved for further analysis.

5) *Open Field Test*: Mice were always placed at the periphery of an open-field arena (40 cm \times 40 cm). The mice were allowed to explore their surroundings freely. The open field was divided into the central area and the peripheral area. A video-tracking system was used to measure mice's spontaneous activity (SMART video-tracking system, Panlab, Spain). Movements were monitored and their behavior was statistically analyzed for 5 min.

6) *Elevated Plus Maze Test*: The EPM apparatus consists of 2 white open arms (30 cm \times 7 cm) perpendicularly conjoined at a center (7 cm \times 7 cm) with two enclosed arms (30 cm \times 7 cm \times 20 cm). Mice were placed in the center zone, with their heads facing open arms, and were allowed to explore freely in darkness and quiet for 5 min for a trial. Video capture software was used to collect the trajectory and behavior indicators of animals. The number of entries and the percentage of travel distance in the open arms were analyzed.

7) *Social Interaction Test*: Mice were allowed to explore the social discrimination chamber (40 \times 40 cm square, 40 cm height) for 2 min with pencil holders (circle with a radius of 7.5 cm and 15 cm height) placed at the upper right and lower left corners of the social discrimination chamber. Following that, the novel conspecific mice were kept in the pencil holders placed at the upper right corner. The test mice were allowed

to explore the chamber for 5 min before returned to home cages. Behavioral tracking was recorded by the camera. The "interaction zone" was defined as the 10 cm area around the pencil holder.

F. In Vivo Fiber Photometry Recording

To avoid interference from ambient light, all behavioral tests were performed under a dark condition with a 3 W lamp facing the ceiling which provides a glimmer for visual demand. The fiber-photometry system (Thinkertech, China) consisted of a 473 nm excitation light from LEDs, reflected off a dichroic mirror with a 435-488 nm reflection band, and coupled into a 200 μ m 0.37 NA optical fiber by an objective lens. We collected emitted fluorescence from targeted brain regions using a single optical fiber while delivering excitation light. Calcium signals were motivated by 470 nm light and signals were collected at a sampling rate of 50 Hz. Before each period of calcium signals recording, the baseline of the environment and mice without mission were recorded. We calculated the normalized change in fluorescence ($\Delta F/F$) by subtracting the baseline fluorescence from the fiber fluorescence at each time point and dividing that value by the baseline fluorescence. The baseline fluorescence was detected 2 s before each social interaction event. Data were aligned by the video recorded simultaneously.

G. Immunofluorescence Staining

Following the calcium signal recording, mice were sacrificed and perfused with saline and 4% paraformaldehyde. The brain tissues were removed and postfixed in 4% paraformaldehyde overnight, followed by gradient dehydration with 15%, and 30% sucrose until the brain tissue completely sank to the bottom. Then, the brains were covered by an embedding medium and sectioned (30 μ m thick) using a freezing microtome (Leica, Germany). The brain slices were permeabilized with 0.3% Triton X-100 in PBS for 10 min and blocked with 5% bovine serum albumin (BSA) in PBS for 1 h. The brain slices were then incubated with the primary antibodies at 4 °C overnight. The primary antibody used was anti-tyrosine hydroxylase (1:200, ab137869, Abcam; 1:400, MAB318, Sigma) and anti-cFos (1:300, 2250, CST). After rinsing three times in PBS for 5 min each, brain slices were incubated with secondary antibodies for 2 h at room temperature in the dark. The secondary antibodies used were goat anti-rabbit IgG H&L (Alexa Fluor 488) (1:1000, ab150081, Abcam), goat anti-mouse IgG H&L (Alexa Fluor 594) (1:1000, ab150120, Abcam), and goat anti-rabbit IgG (Alexa Fluor 647) (1:400, ab150083, Abcam). Nuclei were stained by DAPI. The slices were then photographed with a Nikon fluorescence microscope (Nikon, Japan) to measure the TH⁺ and c-Fos⁺ neurons and verify the expression of the DA-probe and implanted position of the fiber.

H. Statistical Analysis

The numbers of replicates (n) are indicated in the figure legends. All statistical analyses were performed using SPSS,

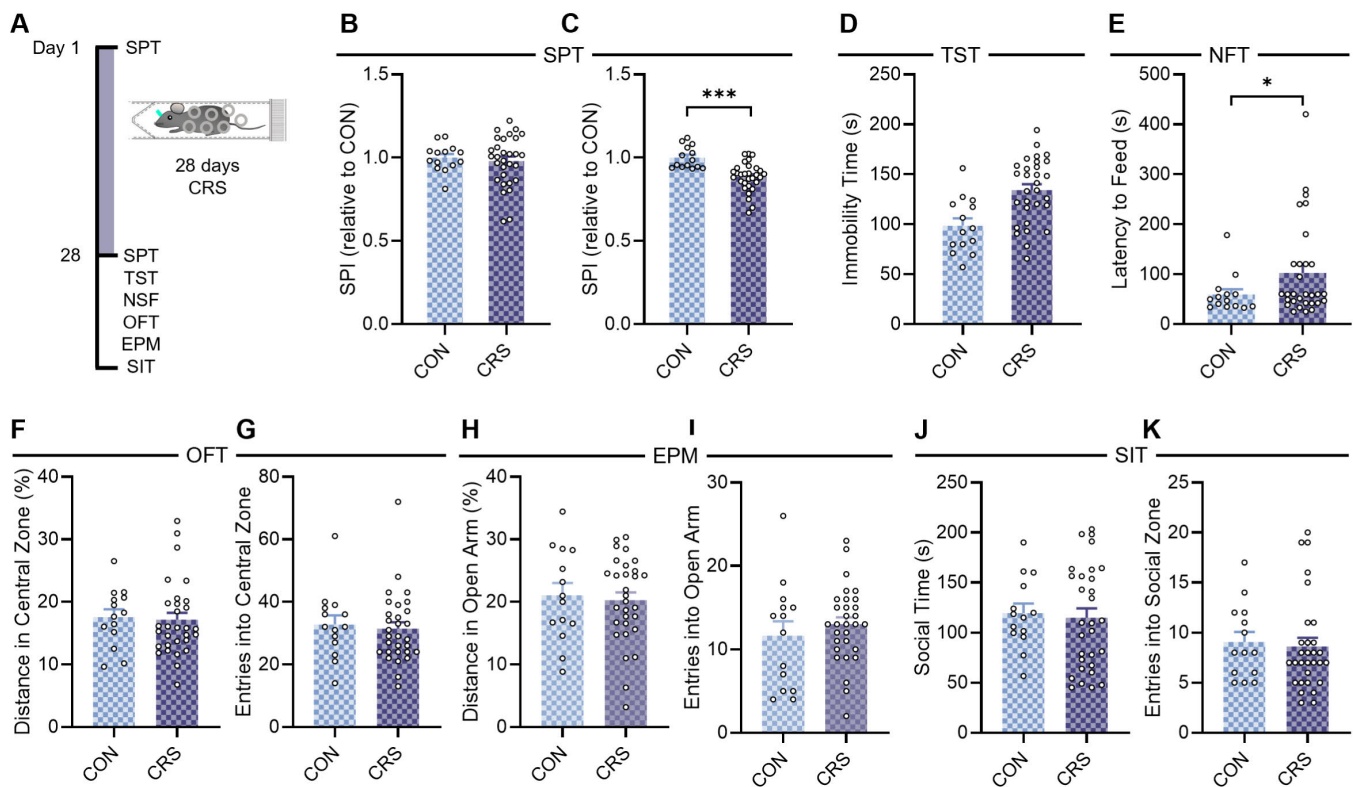


Fig. 1. CRS-induced depression-like behavioral changes in mice. (A) Paradigms of 28-day CRS and behavioral test. (B-C) Sucrose preference index in mice before (B) and after CRS exposure (C). (D) The immobility time in the TST after CRS exposure. (E) The mean latency to feed in the NSF after CRS exposure. (F) The total distance traveled in the open field test. (G) The percentage of distance in the central zone measured in OPT. (H) The mean entries into the central zone in OPT. (I) The mean social time traveled in the SIT. (J) The mean entries into the social zone. n = 14 (control [CON]); n = 30 (chronic restraint stress [CRS]). * $p < 0.05$; ** $p < 0.01$; *** $p < 0.001$.

version 20.0, and GraphPad Prism, version 8.0, with appropriate inferential methods, as indicated in the figure legends. Normally distributed data were tested by unpaired *t*-test for 2-group comparisons and one-way ANOVA followed by LSD's test for multiple comparisons. Repetitive-measure ANOVA was used for the weight data. All data are expressed as mean \pm SEM and statistical significance was set at $p < 0.05$.

III. RESULTS

A. Chronic Restraint Stress Produces Depression-Like Behavior but Not Anxiety-Like Behavior and Social Dysfunction

Chronic restraint stress is a valid rodent model of depression. Mice were assessed for behavioral deficits following the 4-week chronic restraint stress exposure period (Fig. 1A). First, to address whether chronic restraint stress-induced depression-like behaviors, the sucrose preference test, the tail-suspension test (TST), and the novelty-suppressed feeding test (NFT) were used to measure behavioral despair/helplessness. The sucrose-preference test (SPT) was used to measure anhedonia, a core depression symptom. Before CRS exposure, mice were randomly divided into two groups, of which there was no significant difference in sucrose preference index (Fig. 1B, $t_{(42)} = 0.489$, $p = 0.627$). Four-week CRS exposure significantly reduced sucrose preference compared with control mice (Fig. 1C, $t_{(42)} = 4.426$,

$p < 0.001$). Similar to it, in TST the CRS mice showed more immobility time compared with control mice (Fig. 1D, $t_{(42)} = -3.561$, $p = 0.001$). As to the novelty-suppressed feeding test, CRS mice exhibited longer latency to feed compared with control mice (Fig. 1E, $t_{(42)} = -2.132$, $p = 0.039$). These results demonstrated that CRS caused depression-like behavior.

Then we conducted the open-field test (OFT) to assess the anxiety-like behavior of CRS mice. Through measuring the distance (Fig. 1F, $t_{(42)} = 0.237$, $p = 0.814$) and entries (Fig. 1G, $t_{(42)} = 0.372$, $p = 0.711$) in the central zone, CRS mice did not display significantly different compared with the control mice. Similarly, in the EPM test, no difference was found in the percentage of distance traveled in the open arms (Fig. 1H, $t_{(42)} = 0.336$, $p = 0.738$) or the entries into the open arms (Fig. 1I, $t_{(42)} = -0.805$, $p = 0.425$). These results suggested that the CRS mice exhibited normal exploration, without the anxiety behavior. Then the social interaction test (SIT) was conducted to assess the social exploration. Compared to the control mice, the CRS mice traveled similar social time (Fig. 1J, $t_{(42)} = 0.309$, $p = 0.759$) and entries in the social zone (Fig. 1K, $t_{(42)} = 0.307$, $p = 0.761$), suggesting that CRS mice preferred to interact with stranger mice, which was in line with the nature of mice to live in groups.

Together, these results demonstrated that 4-week CRS exposure resulted in depression-like exhibition, but not anxiety-like behavior or social dysfunction.

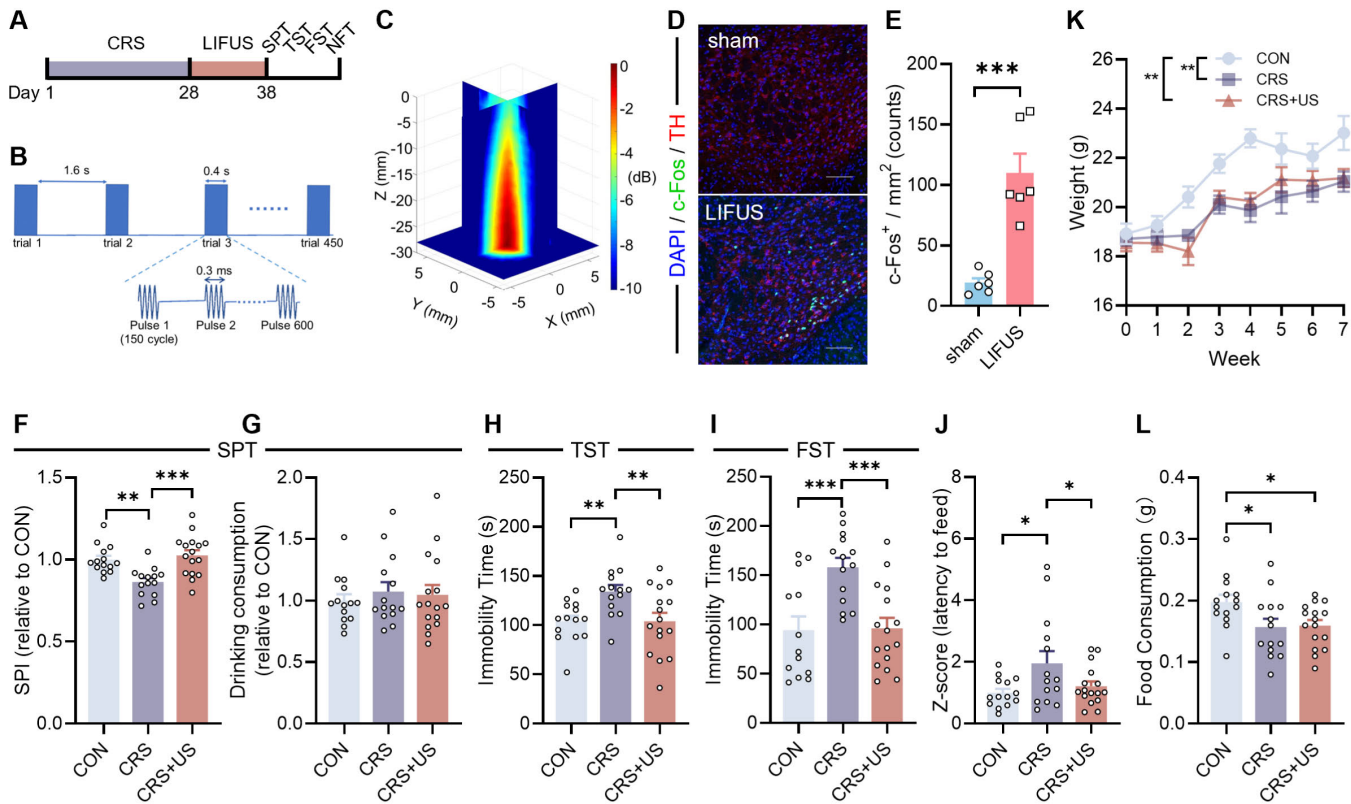


Fig. 2. Low-intensity focused ultrasound stimulation improved the depressive behavior of CRS mice. (A) Paradigms of CRS and US exposure of mice. (B) An illustration of the ultrasound temporal profile used in mice. (C) One transverse (X–Y plane) and sagittal (X–Z plane) scans of ultrasound pressure distribution. (D) Representative images of mouse VTA regions treated with or without LIFUS, stained for c-Fos expression. All scale bars in this panel represent 100 μm . (E) Counts of nuclear c-Fos per slice imaged. N for LIFUS groups = 6 slices from 3 mice and for Sham-LIFUS groups = 6 slices from 3 mice. (F) The z-score of sucrose preference index of the three-group mice. (G) The total drinking consumption of mice during SPT. (H) Immobility time of the three-group mice in the TST. (I) Immobility time of the three-group mice in the FST. (J) The z-score of latency to feed in the NFT. (K) The weight changes of the three-group mice during the whole experiment. (L) In-take food consumption in the home cage for 5 minutes. $n = 14$ (control [CON]); $n = 14$ (chronic restraint stress [CRS]); $n = 16$ (restraint stress with ultrasound stimulation [CRS+US]). * $p < 0.05$; ** $p < 0.01$; *** $p < 0.001$.

B. Low-Intensity Focused Ultrasound Stimulation of the VTA Region Improved the Depression-Like Behaviors of CRS Mice

We then measure whether FUS targeting VTA could improve depression-like behaviors. After 10-day FUS, we measured the SPT firstly to evaluate the anhedonia state (Fig. 2A). The experimental schematic diagram of ultrasound stimulation in the study was as follows (Fig. 2B) and we measured the acoustic field distribution under the simulative condition (Fig. 2C). LIFUS treatment induced greater expression of c-Fos in the nuclei of TH⁺ neurons of VTA region compared with the control VTA region stimulated with Sham-LIFUS (Fig. 2D). c-Fos⁺ cells in the VTA region were more than four times higher in LIFUS mice than in sham LIFUS, showing the neuronal activation following our stimulation strategy (Fig. 2E, $t_{(10)} = -5.559$, $p < 0.001$). Then the LIFUS procedure was performed in the following experiment. During the test stage, there was no significant difference in drinking consumption among the three groups (Fig. 2G, $F_{(2,43)} = 0.261$, $p = 0.772$). However, the sucrose preference index of FUS-treated CRS mice was significantly higher than no-FUS-treated CRS mice (Fig. 2F, $F_{(2,43)} = 10.329$, $p < 0.001$; CON vs. CRS: $p = 0.001$; CRS vs. CRS+US:

$p < 0.001$). Then, TST, NFT, and FST were performed to further measure the behavior performance among the three groups. Both in the TST and FST, FUS-treated CRS mice exhibited lower immobility time (Fig. 2H, $F_{(2,43)} = 6.377$, $p = 0.004$; CON vs. CRS, $p = 0.006$; CRS vs. CRS+US, $p = 0.005$; Fig. 2I, $F_{(2,42)} = 9.473$, $p < 0.001$; CON vs. CRS, $p < 0.001$; CRS vs. CRS+US, $p = 0.003$). The CRS mice under US exposure also exhibited the declined latency to feed in NFT (Fig. 2J, $F_{(2,43)} = 3.759$, $p = 0.032$; CON vs. CRS: $p = 0.013$; CRS vs. CRS+US: $p = 0.042$). Meanwhile, during the whole experiment, we constantly monitored the weight changes of mice. All of them gained weight (Fig. 2K). The CRS mice showed slower growth compared with control mice (Fig. 2K, $F_{(1,41)} = 6.565$, $p = 0.003$; CON vs. CRS: $p = 0.002$; CRS vs. CRS+US: $p = 0.804$; CON vs. CRS+US: $p = 0.004$). Then we weighed the in-cage food consumption of mice for 5 minutes. The results showed that CRS mice eat less than the control group and FUS did not improve the food consumption of CRS mice (Fig. 2L, $F_{(2,43)} = 3.989$, $p = 0.026$, CON vs. CRS: $p = 0.017$; CON vs. FUS: $p = 0.020$). The decreased appetite may result in depressed emotions. These findings suggested that FUS targeting the VTA region could alleviate the depression.

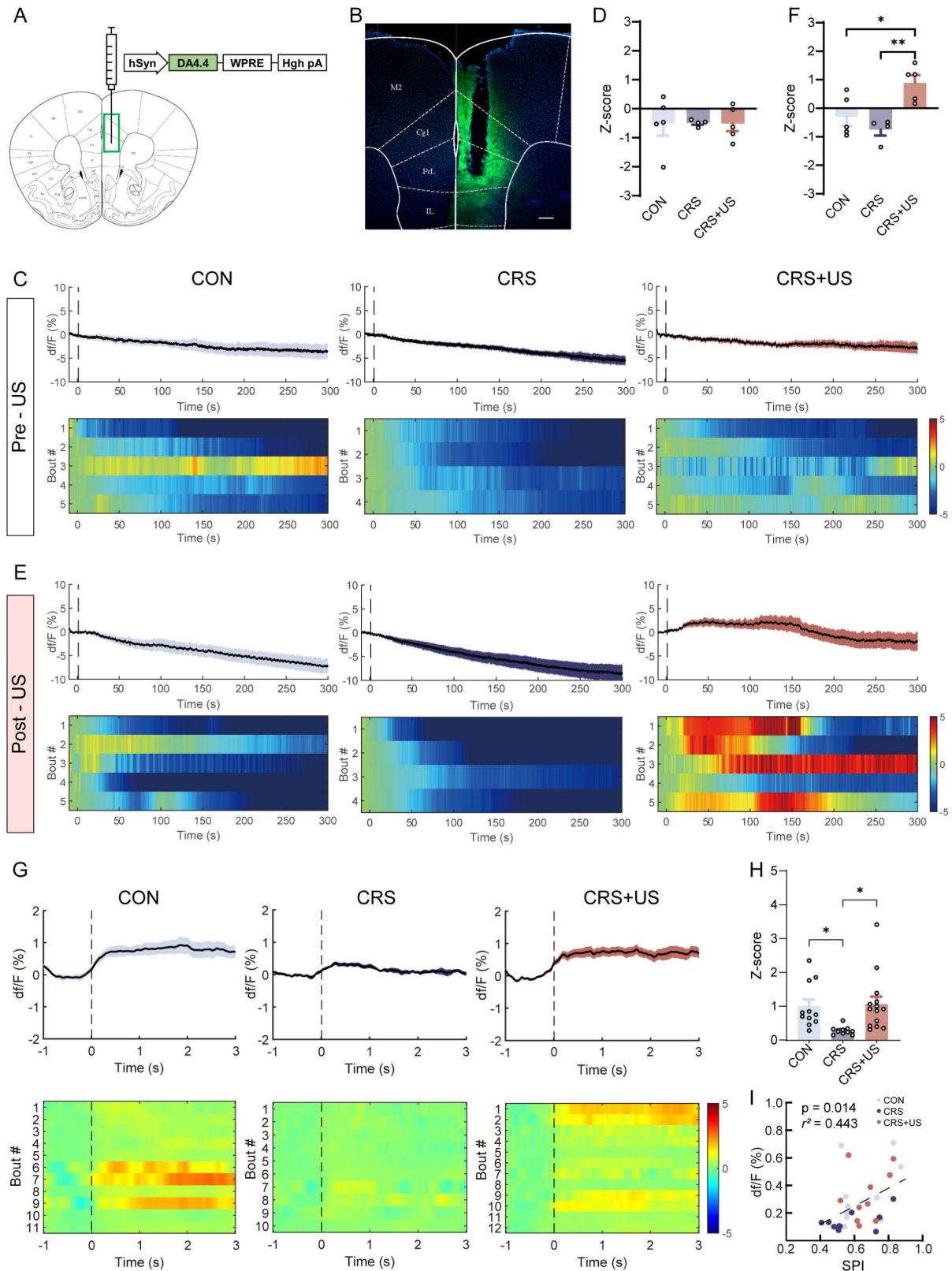


Fig. 3. FUS targeting VTA enables the increase of DA concentration in the mPFC and improves the reward behavior. (A) Schematic of the AAV vector in the mPFC. (B) Representative images of mPFC expressing DA probes, and the dashed box represents the trace of optical fiber. Scale bar: 200µm. (C) Average DA probes fluorescence traces in the mPFC of anesthetized CON, CRS, and CRS+US mice and the average peak DA activity during the 5-min recording (D) before FUS stimulation. (E) In response to the FUS, the average DA probes fluorescence traces in the mPFC of anesthetized CON, CRS, and CRS+US mice and the average peak DA activity (F). $n = 5$ (CON); $n = 4$ (CRS); $n = 5$ (CRS+US). * $p < 0.05$; ** $p < 0.01$. (G) Averaged dopamine fluorescence signal change (df/F) in the mPFC of CON, CRS, and CRS+US mice. The dotted line shows the timing of licking sucrose water. (H) Average z-score of dopamine activity in response to sucrose water. $n = 11$ (CON); $n = 10$ (CRS); $n = 14$ (CRS+US). (I) Relationship between z score of dopamine signal and sucrose preference index (SPI). $n = 10$ (CON); $n = 10$ (CRS); $n = 10$ (CRS+US). * $p < 0.05$.

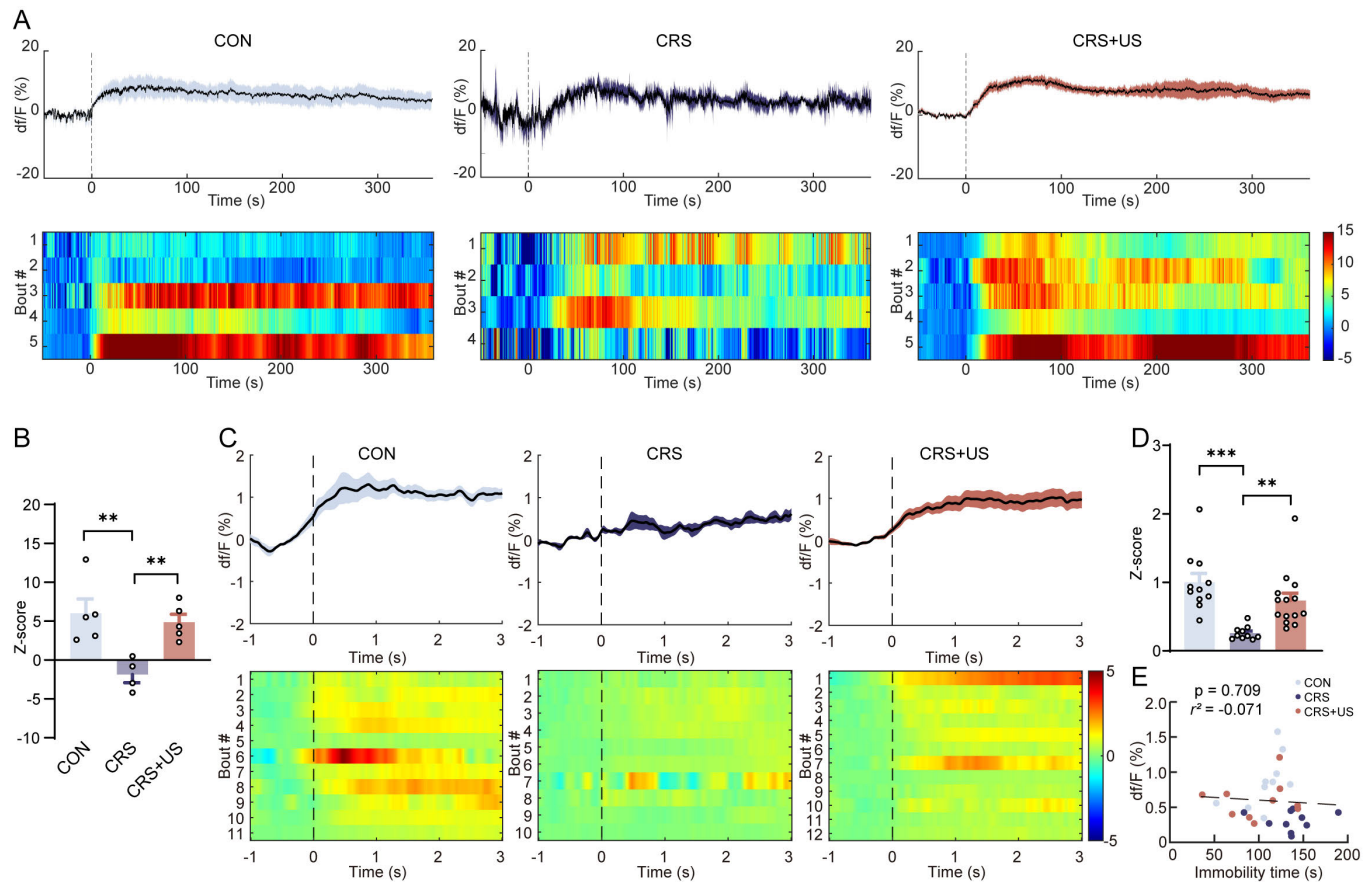


Fig. 4. FUS enhanced the dopamine concentration in the mPFC during the struggling of CRS mice. (A and B) Time course and representative heatmaps of dopamine fluorescence z scores in the mPFC of three-group mice during the 5-min TST (A) and quantification of the average mean z score during TST (B). The black line represents the mean dF/F of the dopamine signal. $n = 5$ (CON); $n = 4$ (CRS); $n = 5$ (CRS+US). (C) Representative plot showing the average dopamine fluorescence signal change aligned to the start of struggling behavior. The dotted line shows the timing of struggling. (D) Average z-score of dopamine activity in response to sucrose water. $n = 11$ (CON); $n = 10$ (CRS); $n = 14$ (CRS+US). (E) Relationship between z score of dopamine signal and the immobility time in TST. $n = 10$ (CON); $n = 10$ (CRS); $n = 10$ (CRS+US). ** $p < 0.01$, *** $p < 0.001$.

C. FUS Targeting VTA Increased the DA Release in mPFC and Mediated the CRS-Induced Reward Behavior

We next investigated the role of FUS targeting VTA in the regulation of depression-like behavior. The VTA is a midbrain reward center, where the dopaminergic (DA) circuit is well-defined and involved in various reward-related behavior and diseases. To test whether VTA-mPFC DA projection has increased dopamine concentration. We next recorded the DA signals through the DA probes (GPCR-activation-base-DA) to evaluate the DA expression and observed robust expression of GFP in mPFC. The optical fiber was implanted in the PrL region of mPFC (Fig. 3A-B). Before the ultrasound stimulation, 5-min fluorescence was recorded continuously (Fig. 3C). The fluorescence curve of control mice showed a decreasing trend, perhaps due to the photobleaching property of fluorescence (Fig. 3C). Then the DA signals were measured by the average dF/F in 5 minutes and there was no significant difference in the mean intensity of dF/F among the three groups (Fig. 3D, $F_{(2,14)} = 0.239$, $p = 0.791$). Then we recorded and analyzed the instant response of DA signals to the FUS (Fig. 3E). During the FUS procedure, the first 5-min dopamine signal was analyzed. Similarly, the signal in CON and CRS groups exhibited a declining trend and the CRS mice exposed

to FUS showed an upward tendency (Fig. 3E). However, the CRS mice receiving FUS exhibited an increasing change since the FUS procedure, which was not found in CRS sham-FUS mice (Fig. 3F, $F_{(2,14)} = 8.696$, $p = 0.005$; CON vs. CRS: $p = 0.285$; CRS vs. CRS+FUS: $p = 0.002$; CON vs. CRS+FUS: $p = 0.012$). Taken together, these results suggested that FUS targeting VTA can increase the DA concentration in the mPFC.

According to the behavioral performance, FUS improved the CRS-induced reward loss. We next tested whether the improvement of reward behavior was related to the mPFC dopamine release. After 24-h fasting and water deprivation, sucrose water was considered as a reward to experimental mice. During the licking stage, we recorded the DA concentration of mPFC in half an hour. The licking time was measured by a customer sensor and we analyzed the following 1-s window signal. We observed an increased fluorescence signal in CON mice, while the CRS mice exhibited a relative plate curve (Fig. 3G). Then the mean dF/F (z-score) was calculated to evaluate it and we found that FUS enhanced the response of CRS mice to rewarding (Fig. 3H, $F_{(2,32)} = 4.824$, $p = 0.015$; CON vs. CRS: $p = 0.017$; CRS vs. CRS+FUS: $p = 0.007$; CON vs. CRS+FUS: $p = 0.811$). Meanwhile, the

dopamine signal in the mPFC and sucrose preference index were positively correlated (Fig. 3I, Pearson's correlation coefficient, $r^2 = 0.443$, $p = 0.014$). Thus, these findings showed that FUS-induced enhancement of mPFC dopamine release mediated the CRS-induced reward loss.

D. FUS Treatment Decreased the Despair Behavior Induced by CRS Exposure

Apart from the reward behavior, motivation and despair also belong to the core symptoms of depression. Based on the decrease of immobile behavior in TST, we then measured the change of dopamine concentration during the struggle considered as survival motivation. We recorded the fluorescence signal in the whole 6-min TST. Firstly, we analyzed the signal during the whole test stage. According to the heat map, the rising trend of the signal was observed in CON and CRS+FUS mice (Fig. 4A), while the dopamine signal of CRS mice exhibited a relatively steady change (Fig. 4A). The average intensity of dopamine fluorescence also showed the same result (Fig. 4B, $F_{(2,11)} = 8.390$, $p = 0.006$; CON vs. CRS: $p = 0.003$; CRS vs. CRS+FUS: $p = 0.07$; CON vs. CRS+FUS: $p = 0.567$). Further, the temporal signal response in each struggle was measured. When the CON mice struggled, the dopamine signal elevation appeared (Fig. 4C). But compared to the CON mice, there was a very small rise in the CRS mice, which was reversed by FUS targeting VTA to some extent (Fig. 4C). After analyzing the 3-s average value and peak value in each struggle, we obtained the consistent results. There was a significant decrease in dopamine concentration in the mPFC of CRS-exposure mice (Fig. 4D, $F_{(2,32)} = 11.404$, $p < 0.001$; CON vs. CRS: $p < 0.001$; CRS vs. CRS+FUS: $p = 0.003$; CON vs. CRS+FUS: $p = 0.075$). However, there was no significant association between the dopamine signal in the mPFC and immobility in TST (Pearson's correlation coefficient, $r^2 = 0.071$; $p = 0.709$) (Fig. 4E). These results indicated that FUS stimulating VTA improved the dopamine concentration of mPFC during struggling, which may be resulted in blocking the despair behavior.

E. CRS Modeling Impaired the VTA DA Neuron

The VTA is involved in emotion-related behaviors, in which dopamine neurons are mainly located. The dopamine of mPFC is mainly from the VTA-projecting dopaminergic neuron. Thus, whether the VTA neuron damage decreased the dopamine level in mPFC and affected the depression-like behavior? Thus, we examined the neuron labeled tyrosine hydroxylase (TH), a marker for dopaminergic neurons (Fig. 5A). The image showed that there was a significant decrease in the number of TH-positive neurons in the VTA area compared with control mice (Fig. 5B, $F_{(2,33)} = 5.590$, $p = 0.008$; CON vs. CRS: $p = 0.006$; CRS vs. CRS+FUS: $p = 0.007$; CON vs. CRS+FUS: $p = 0.951$). We next measured the morphology of neurons in VTA and mPFC. Through HE staining, in the control mice, cells exhibited regular and compact arrangement in the VTA area, with the cytoplasm stained and well-distributed, suggesting that no obvious cell damage was seen (Fig. 5C). In the CRS group, neuron loss,

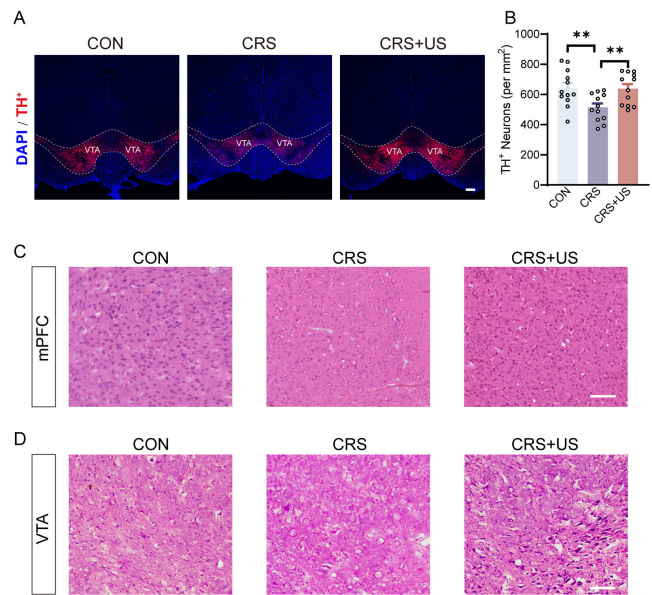


Fig. 5. The morphological changes of the neuron in VTA and mPFC regions. (A) Immunostaining for TH⁺ neuron in VTA region ($n = 12$ view from 3 mice in each group). The dotted lines indicate the VTA region. Scale bar: 200 μm . (B) Quantification of the TH-positive neuron in VTA of three-group mice. (C and D) Typical diagrams of HE staining in VTA (C) and mPFC area (D) of three-group mice. Scale bar: 100 μm . ** $p < 0.01$.

shrinkage, and loose arrangement were observed, whereas these were all reversed after FUS (Fig. 5C). The similar phenomenon was observed in the mPFC region (Fig. 5D). The above findings showed that FUS targeting VTA can enhance the survival ability of neuron in VTA and mPFC of CRS mice, especially the DA neuron in VTA.

IV. DISCUSSION

In this study, we revealed that focused ultrasound stimulation targeting VTA improved the depression-like behavior induced by chronic restraint stress, and the dopamine level of mPFC can be enhanced by FUS. Furthermore, our results demonstrated that FUS treatment alleviated CRS-induced anhedonia and despair by protecting the dopaminergic neurons in VTA and enhancing the downstream dopamine level in mPFC.

Chronic stress raises the incidence level of depression. Although male rodents are more commonly used in the model of depression, some studies report that female mice also show stable changes in depression-like behaviors and biological indicators [21]. In addition, women are nearly twice as likely as men to be diagnosed with depression, and the response to chronic stress in female mice is greater than that in male mice [22], [23], [24]. Thus, in this study, female mice were chosen to do the experiment undergoing chronic restraint stress. Our study confirmed that CRS exposure would induce depression-related symptoms as indicated by the SPT, TST, and NFT, which was by the previous study [25], [26]. In addition, our results showed that after exposure to CRS for 4 weeks, mice did not exhibit anxious-related behavior evaluated by OPT or social interaction, inconsistent with the previous study [26]. One reason for this discrepancy might

be attributed to the total duration of CRS. Wang et al. applied restraint stress 3 hours daily for 10 days, whereas we administered restraint stress 4 hours daily for 28 days. Other differences in experimental procedures may be due to the gender differences in depression, and more study is required to understand the potential effect.

As previously reported, major depression disorder usually occurs with the dysfunction of the dopamine system [27]. And chronic stress-induced depressive behavior along with the declined dopamine level in mPFC [2]; meanwhile, enhancing the dopamine level in mPFC reversed the depression behavior [28]. Here, we aimed to suggest how the dopamine level in mPFC changed during abnormal behaviors. Our results showed that CRS-induced anhedonia and despair along with the declined dopamine level of mPFC. The dopamine of mPFC mainly comes from VTA, which contains a mixture of dopaminergic (~65%) neurons [7]. The dopamine signaling in VTA projection targets, such as the mPFC, may promote the initiation and maintenance of reward-seeking behaviors in VTA. Thus, activating the VTA may increase the dopamine level of mPFC to improve depression-like behaviors. The previous research and our recent study showed that focused ultrasound stimulation can activate the neurons [16], [19]. Here, we applied the focused ultrasound stimulation to VTA in this study to investigate the therapeutic effect and DA level in mPFC. In our previous study we performed the LIFUS targeting mPFC and the results showed that the LIFUS strategy used can increase the neuronal activity of mPFC [16]. In this study, we aimed to excite the DAergic neurons in the VTA region and then increase the downstream dopamine level. Thus, we increased the stimulation intensity based on previous parameters [16]. Through the DA probe, we measured the DA signal and found that 5-min FUS could indeed increase the DA level of mPFC.

Then we measured the effect of FUS on two of the hallmark symptoms of depression-anhedonia and despair. The results showed that FUS targeting VTA rescued the decreased sucrose preference and immobility induced by chronic restraint stress. Along with the improvement of behavior, the dopamine level in mPFC also increased following ultrasound stimulation. The previous study reported that during the reward behavior, resilient individuals have behavioral strategies and behavior-aligned DA neural activity dynamics that differentiate them from susceptible individuals [6]. Here, we found when the mice licked the sucrose water, the more the SPI was, the higher the z score of dopamine signal was in mPFC. There was a positive correlation between the SPI and DA signal, which suggested that the dopamine level in mPFC was indeed involved in the anhedonia of depression. However, regarding the despair behavior, the DA level was not correlated with the immobility time in TST. It may be due to that the different mPFC regions aid in the different regulation of specific behaviors. Previous investigations have established that specific prefrontal subregions, such as the prelimbic (PL) and infralimbic (IL) cortex, are involved in the service of avoiding aversive outcomes or obtaining rewarding ones [29].

Accumulating studies implicated that chronic stress causes structural remodeling in the brain structures [30], [31]. VTA

dopaminergic neurons were impaired after the stress exposure. Here, compared with the non-CRS mice, the morphology and arrangement of VTA cells in CRS mice were impaired. We further measured the number of TH+ neurons and found that FUS targeting VTA improved the DA neurons impaired by CRS exposure. Furthermore, prefrontal cortical pyramidal cells that receive dopamine afferents often display a synaptic architecture, and the lesions of the VTA DAergic neurons projecting to PFC lead to dendritic spine loss [32]. Structural atrophy such as spine density retraction in the PFC can be observed as an effect of stress exposure [16]. Then, whether the protection of VTA DAergic neurons affect the cells in mPFC? Through the HE staining, we observed the improvement of neurons in mPFC induced by CRS, in line with the previous report on the impairment of neuronal activity in mPFC after chronic stress [16].

In summary, we demonstrated that targeting VTA FUS treatment significantly rescued the depressive-like behavior and declined dopamine level of mPFC induced by CRS. These beneficial effects of FUS might be due to protection in the DA neuron of VTA. Our findings suggest that FUS treatment could serve as a new therapeutic strategy for the treatment of stress and associated diseases. Further investigations are needed, however, to evaluate the mechanism of FUS in the protection of neurons.

REFERENCES

- [1] X.-J. Kuang et al., "P2X2 receptors in pyramidal neurons are critical for regulating vulnerability to chronic stress," *Theranostics*, vol. 12, no. 8, pp. 3703–3718, 2022, doi: [10.7150/thno.72144](https://doi.org/10.7150/thno.72144).
- [2] E. Venzala, A. L. García-García, N. Elizalde, and R. M. Tordera, "Social vs. environmental stress models of depression from a behavioural and neurochemical approach," *Eur. Neuropsychopharmacol.*, vol. 23, no. 7, pp. 697–708, Jul. 2013, doi: [10.1016/j.euroneuro.2012.05.010](https://doi.org/10.1016/j.euroneuro.2012.05.010).
- [3] J. Fan et al., "O-GlcNAc transferase in astrocytes modulates depression-related stress susceptibility through glutamatergic synaptic transmission," *J. Clin. Invest.*, vol. 133, no. 7, Apr. 2023, Art. no. e160016, doi: [10.1172/jci160016](https://doi.org/10.1172/jci160016).
- [4] J.-H. Baik, "Stress and the dopaminergic reward system," *Experim. Mol. Med.*, vol. 52, no. 12, pp. 1879–1890, Dec. 2020, doi: [10.1038/s12276-020-00532-4](https://doi.org/10.1038/s12276-020-00532-4).
- [5] K. M. Tye et al., "Dopamine neurons modulate neural encoding and expression of depression-related behaviour," *Nature*, vol. 493, no. 7433, pp. 537–541, Jan. 2013, doi: [10.1038/nature11740](https://doi.org/10.1038/nature11740).
- [6] L. Willmore, C. Cameron, J. Yang, I. B. Witten, and A. L. Falkner, "Behavioural and dopaminergic signatures of resilience," *Nature*, vol. 611, no. 7934, pp. 124–132, 2022, doi: [10.1038/s41586-022-05328-2](https://doi.org/10.1038/s41586-022-05328-2).
- [7] R. van Zessen, J. L. Phillips, E. A. Budygin, and G. D. Stuber, "Activation of VTA GABA neurons disrupts reward consumption," *Neuron*, vol. 73, no. 6, pp. 1184–1194, Mar. 2012, doi: [10.1016/j.neuron.2012.02.016](https://doi.org/10.1016/j.neuron.2012.02.016).
- [8] K. Z. Peters and F. Naneix, "The role of dopamine and endocannabinoid systems in prefrontal cortex development: Adolescence as a critical period," *Frontiers Neural Circuits*, vol. 16, Nov. 2022, Art. no. 939235, doi: [10.3389/fncir.2022.939235](https://doi.org/10.3389/fncir.2022.939235).
- [9] S. J. Russo and E. J. Nestler, "The brain reward circuitry in mood disorders," *Nature Rev. Neurosci.*, vol. 14, no. 9, pp. 609–625, Sep. 2013, doi: [10.1038/nrn3381](https://doi.org/10.1038/nrn3381).
- [10] E. Lee et al., "Enhanced neuronal activity in the medial prefrontal cortex during social approach behavior," *J. Neurosci.*, vol. 36, no. 26, pp. 6926–6936, Jun. 2016, doi: [10.1523/jneurosci.0307-16.2016](https://doi.org/10.1523/jneurosci.0307-16.2016).
- [11] A. C. Brumback et al., "Identifying specific prefrontal neurons that contribute to autism-associated abnormalities in physiology and social behavior," *Mol. Psychiatry*, vol. 23, no. 10, pp. 2078–2089, Oct. 2018, doi: [10.1038/mp.2017.213](https://doi.org/10.1038/mp.2017.213).

- [12] Q. Li et al., "Oxytocin exerts antidepressant-like effect by potentiating dopaminergic synaptic transmission in the mPFC," *Neuropharmacology*, vol. 162, Jan. 2020, Art. no. 107836, doi: [10.1016/j.neuropharm.2019.107836](https://doi.org/10.1016/j.neuropharm.2019.107836).
- [13] Q. Xian et al., "Modulation of deep neural circuits with sonogenetics," *Proc. Nat. Acad. Sci. USA*, vol. 120, no. 22, May 2023, Art. no. e2220575120, doi: [10.1073/pnas.2220575120](https://doi.org/10.1073/pnas.2220575120).
- [14] D. Dalecki, "Mechanical bioeffects of ultrasound," *Annu. Rev. Biomed. Eng.*, vol. 6, no. 1, pp. 229–248, Aug. 2004, doi: [10.1146/annurev.bioeng.6.040803.140126](https://doi.org/10.1146/annurev.bioeng.6.040803.140126).
- [15] K. Yu, X. Niu, E. Krook-Magnuson, and B. He, "Intrinsic functional neuron-type selectivity of transcranial focused ultrasound neuromodulation," *Nature Commun.*, vol. 12, no. 1, p. 2519, May 2021, doi: [10.1038/s41467-021-22743-7](https://doi.org/10.1038/s41467-021-22743-7).
- [16] Y. Wang et al., "Low-intensity focused ultrasound stimulation reverses social avoidance behavior in mice experiencing social defeat stress," *Cerebral Cortex*, vol. 32, no. 24, pp. 5580–5596, Dec. 2022, doi: [10.1093/cercor/bhac037](https://doi.org/10.1093/cercor/bhac037).
- [17] J. Wang et al., "Transcranial focused ultrasound stimulation improves neurorehabilitation after middle cerebral artery occlusion in mice," *Aging Disease*, vol. 12, no. 1, pp. 50–60, Feb. 2021, doi: [10.14336/ad.2020.0623](https://doi.org/10.14336/ad.2020.0623).
- [18] Y. Yuan, Z. Zhao, Z. Wang, X. Wang, J. Yan, and X. Li, "The effect of low-intensity transcranial ultrasound stimulation on behavior in a mouse model of Parkinson's disease induced by MPTP," *IEEE Trans. Neural Syst. Rehabil. Eng.*, vol. 28, no. 4, pp. 1017–1021, Apr. 2020, doi: [10.1109/TNSRE.2020.2978865](https://doi.org/10.1109/TNSRE.2020.2978865).
- [19] Y. Tufail et al., "Transcranial pulsed ultrasound stimulates intact brain circuits," *Neuron*, vol. 66, no. 5, pp. 681–694, Jun. 2010, doi: [10.1016/j.neuron.2010.05.008](https://doi.org/10.1016/j.neuron.2010.05.008).
- [20] J. Lim et al., "ASIC1a is required for neuronal activation via low-intensity ultrasound stimulation in mouse brain," *eLife*, vol. 10, Sep. 2021, Art. no. e61660, doi: [10.7554/eLife.61660](https://doi.org/10.7554/eLife.61660).
- [21] S. Jiang, L. Lin, L. Guan, and Y. Wu, "Selection of the male or female sex in chronic unpredictable mild stress-induced animal models of depression," *BioMed Res. Int.*, vol. 2022, pp. 1–8, Jun. 2022, doi: [10.1155/2022/2602276](https://doi.org/10.1155/2022/2602276).
- [22] R. H. Salk, J. S. Hyde, and L. Y. Abramson, "Gender differences in depression in representative national samples: Meta-analyses of diagnoses and symptoms," *Psychol. Bull.*, vol. 143, no. 8, pp. 783–822, Aug. 2017, doi: [10.1037/bul0000102](https://doi.org/10.1037/bul0000102).
- [23] M. Rincón-Cortés and A. A. Grace, "Sex-dependent effects of stress on immobility behavior and VTA dopamine neuron activity: Modulation by ketamine," *Int. J. Neuropsychopharmacol.*, vol. 20, no. 10, pp. 823–832, Oct. 2017, doi: [10.1093/ijnp/pyx048](https://doi.org/10.1093/ijnp/pyx048).
- [24] C. Bouarab et al., "Sex-specific adaptations to VTA circuits following subchronic stress," *BioRxiv*, Aug. 2023, Art. no. 551665, doi: [10.1101/2023.08.02.551665](https://doi.org/10.1101/2023.08.02.551665).
- [25] M. Zhang et al., "Dysfunction of GluN3A subunit is involved in depression-like behaviors through synaptic deficits," *J. Affect. Disorders*, vol. 332, pp. 72–82, Jul. 2023, doi: [10.1016/j.jad.2023.03.076](https://doi.org/10.1016/j.jad.2023.03.076).
- [26] S. Wang et al., "Agarwood essential oil ameliorates restrain stress-induced anxiety and depression by inhibiting HPA axis hyperactivity," *Int. J. Mol. Sci.*, vol. 19, no. 11, p. 3468, Nov. 2018, doi: [10.3390/ijms19113468](https://doi.org/10.3390/ijms19113468).
- [27] Y. Li et al., "Dopamine-mediated major depressive disorder in the neural circuit of ventral tegmental area-nucleus accumbens-medial prefrontal cortex: From biological evidence to computational models," *Frontiers Cellular Neurosci.*, vol. 16, Jul. 2022, Art. no. 923039, doi: [10.3389/fncel.2022.923039](https://doi.org/10.3389/fncel.2022.923039).
- [28] J. Li et al., "SNRIs achieve faster antidepressant effects than SSRIs by elevating the concentrations of dopamine in the fore-brain," *Neuropharmacology*, vol. 177, Oct. 2020, Art. no. 108237, doi: [10.1016/j.neuropharm.2020.108237](https://doi.org/10.1016/j.neuropharm.2020.108237).
- [29] G. Capuzzo and S. B. Floresco, "Prelimbic and infralimbic prefrontal regulation of active and inhibitory avoidance and reward-seeking," *J. Neurosci.*, vol. 40, no. 24, pp. 4773–4787, Jun. 2020, doi: [10.1523/jneurosci.0414-20.2020](https://doi.org/10.1523/jneurosci.0414-20.2020).
- [30] C. Liston et al., "Stress-induced alterations in prefrontal cortical dendritic morphology predict selective impairments in perceptual attentional set-shifting," *J. Neurosci.*, vol. 26, no. 30, pp. 7870–7874, Jul. 2006, doi: [10.1523/jneurosci.1184-06.2006](https://doi.org/10.1523/jneurosci.1184-06.2006).
- [31] B. Czéh et al., "Chronic social stress inhibits cell proliferation in the adult medial prefrontal cortex: Hemispheric asymmetry and reversal by fluoxetine treatment," *Neuropsychopharmacology*, vol. 32, no. 7, pp. 1490–1503, Jul. 2007, doi: [10.1038/sj.npp.1301275](https://doi.org/10.1038/sj.npp.1301275).
- [32] H.-D. Wang and A. Y. Deutch, "Dopamine depletion of the prefrontal cortex induces dendritic spine loss: Reversal by atypical antipsychotic drug treatment," *Neuropsychopharmacology*, vol. 33, no. 6, pp. 1276–1286, May 2008, doi: [10.1038/sj.npp.1301521](https://doi.org/10.1038/sj.npp.1301521).